Complete spectroscopy of ^{211}Po below 2.0 MeV via the (α, n) reaction

J. R. Cottle,[1] Vandana Tripathi,[2] B. A. Brown,[3,4] B. Abromeit,[2] J. M. Allmond,[5] M. Anastasiou,[2] L. T. Baby,[2] J. S. Baron,[2] P. D. Cottle,[2] R. Dungan,[2] T. C. Hensley,[2] K. W. Kemper,[2] R. S. Lubna,[2] N. Rijal,[2] E. Rubino,[2] S. L. Tabor,[2] P.-L. Tai,[2] K. Villafana,[2] and I. Wiedenhoever[2]

[1]*Department of Physics, Grinnell College, Grinnell, Iowa 50112, USA*

[2]*Department of Physics, Florida State University, Tallahassee, Florida 32306, USA*

[3]*National Superconducting Cyclotron Laboratory, Michigan State University, East Lansing, Michigan 48824, USA*

[4]*Department of Physics and Astronomy, Michigan State University, East Lansing, Michigan 48824, USA*

[5]*Physics Division, Oak Ridge National Laboratory, Oak Ridge, Tennessee 37831, USA*

(Received 9 February 2017; published 23 June 2017)

We report the results of a γ-ray spectroscopic study of ^{211}Po via the ^{208}Pb(α,n) reaction at 24-MeV incident energy using a thick target. We observe 26 new γ rays, allowing us to identify 18 states that were not observed in previous γ-ray studies. In total, we observe 45 states below 2.0 MeV. A shell model calculation using the modified Kuo-Herling interaction developed by Warburton and Brown predicts 46 states below 2.0 MeV having spins of 21/2 and below, demonstrating the power of this calculation to provide detailed nuclear structure information on nuclei in the vicinity of ^{208}Pb.

DOI: 10.1103/PhysRevC.95.064323

I. INTRODUCTION

The isotopes in the neighborhood of ^{208}Pb have provided an excellent laboratory for the development and testing of the nuclear shell model. However, for some of these isotopes, such as the three-valence-nucleon isotope ^{211}Po that is the subject of the present work, the density of states becomes large at a relatively low energy. This makes the customary detailed state-by-state comparison between theory and experiment impractical above a certain excitation energy.

In the present work, we implement a novel test of a shell-model calculation using the modified Kuo-Herling interaction developed by Warburton and Brown [1]. We use the reaction (α,n), which has been shown to provide complete spectroscopy by Dewald *et al.* [2], to measure the number of states that occur in the range of excitation energy and spin accessible to the reaction. We then see if the shell-model calculation can reproduce the number of observed states.

We performed a γ-ray spectroscopy study of the ^{208}Pb(α,n)^{211}Po reaction with a beam energy of 24 MeV and a thick target. We observed 26 γ rays that were not observed in either a previous study of the ^{208}Pb(α,n)^{211}Po reaction [3] or another γ ray study of ^{211}Po using light heavy-ion reactions [4]. The present experiment established the existence of at least 18 states that have not been observed in the earlier two γ-ray studies.

II. EXPERIMENTAL DETAILS

The experiment was run at the John D. Fox Superconducting Accelerator Laboratory at Florida State University (FSU). A 24-MeV beam of α particles that was produced by the facility's FN Tandem Van de Graaf accelerator impinged on a thick (50 mg/cm^2) target of enriched ^{208}Pb. The beam energy was chosen to maximize the cross section for populating the states of interest in ^{211}Po while keeping the contamination by the 2n evaporation channel (^{210}Po) low.

The γ rays produced in the reaction were detected with an array of seven Ge detectors. Six of these detectors were of the clover design, of which only three were Compton-suppressed. The seventh detector was a Compton-suppressed single-crystal detector of 80% relative efficiency. Five of the detectors were located at an angle of 90 deg to the beam direction, and the others were located at 135 deg.

The three unsuppressed clover detectors are part of the Clarion array at Oak Ridge National Laboratory and were loaned to FSU.

The data were acquired by a Digital Gamma Finder Pixie 16 system. The coincidence and Compton suppression logic was performed by custom firmware in the digitizer. The coincidence condition was set to require two γ rays arriving together. The leading-edge time stamps were corrected for energy walk. During the experiment, 671.5 million coincidence events were collected.

The data were analyzed using the software GNUSCOPE [5]. The data were sorted for events in which two γ rays were detected within the specified time window into a two-dimensional matrix. From the matrix, γ rays in coincidence with a particular transition of interest allowed us to build the level structure.

III. EXPERIMENTAL RESULTS

The analysis focused on twofold coincidences. We examined coincidence spectra gated on seven previously observed transitions in ^{211}Po that deexcite directly to the ground state and do not occur strongly in ^{210}Po, which is the strongest competing channel in the α + ^{208}Pb reaction via (α,2n). These seven transitions are 687.0, 1050.9, 1064.3, 1121.8, 1160.1, 1409.6, and 1436.6 keV. A γ-ray spectrum gated on each of these seven "clean" ground-state transitions was produced. For each γ ray observed in one of the clean ground-state transition gates, a coincidence spectrum gated on that γ ray was produced. A γ ray was placed in the ^{211}Po level scheme

TABLE I. γ rays observed in the present study.

Gate [keV]	E_γ [keV]	New γ ray	I_γ	E_{initial} [keV]	E_{final} [keV]
687.0	114.5(3)		0.45(3)	1541.8	1427.3
	189.1(3)		2.40(12)	1616.4	1427.3
	268.9(3)		2.48(12)	1696.2	1427.3
	277.8(3)		6.35(32)	1459.2	1181.4
	308.9(3)		2.01(10)	1736.2+x	1427.3+x
	363.0(3)		62.4(31)	1427.3	1064.5
	377.8(3)		67.2(34)	1064.5	687.0
	424.6(3)		0.98(7)	1851.9	1427.3
	475.0(3)		12.6(6)	1902.3+x	1427.3+x
	488.2(3)		3.19(16)	1915.5	1427.3
	494.1(3)		25.9(13)	1181.4	687.0
	511.8(3)		76.0(38)	1939.1+x	1427.3+x
	569.6(3)	Y	9.17(46)	1633.9	1064.5
	665.8(3)		4.97(25)	2093.1	1427.3
	790.7(3)		2.64(14)	2218.0	1427.3
	853.8(3)	Y	14.1(7)	1918.0	1064.5
	925.1(3)		3.30(17)	2352.4	1427.3
	1015.1(3)		16.1(8)	2442.4+x	1427.3+x
	1028.7(3)		91.7(46)	1715.7	687.0
	1039.8(3)		71.5(36)	1726.8	687.0
	1110.4(3)		82.1(41)	1797.4	687.0
	1123.0(3)		60.2(30)	1810.0	687.0
	1190.0(3)		56.0(28)	1877.2	687.0
	1257.4(3)		100(5)	1944.7	687.0
1050.9	171.5(3)		2.21(11)	1614.8	1443.5
	193.2(3)		29.3(15)	1578.5	1385.3
	296.6(3)		6.93(35)	1740.0	1443.5
	334.4(3)		96.8(48)	1385.3	1050.9
	354.7(3)		12.9(6)S	1740.0	1385.3
	355.0(3)		12.9(6)S	2094.8	1740.1
	392.6(3)		100(5)	1443.5	1050.9
	457.9(3)		8.79(44)	1508.8	1050.9
	533.7(3)		20.9(10)	1584.6	1050.9
	563.9(3)		24.6(12)	1614.8	1050.9
	587.4(3)	Y	9.00(45)	1638.0	1050.9
	596.2(3)	Y	9.15(46)	1647.1	1050.9
	645.6(3)		18.6(9)	2224.1	1578.5
	651.1(3)		8.10(41)	2094.8	1443.5
	668.7(3)		3.21(16)	2112.1	1443.5
	738.7(3)	Y	6.63(33)	1789.6	1050.9
	854.6(3)		22.3(11)	2298.1	1443.5
	896.2(3)		12.6(6)	2339.7	1443.5
	915.3(3)		9.17(5)	2300.6	1443.5
	969.2(3)		11.5(6)	2547.7	1578.5
	973.9(3)		32.7(16)	2024.8	1050.9
	983.0(3)		24.4(12)	2033.9	1050.9
	1014.3(3)	Y	7.91(40)	2065.2	1050.9
	1026.7(3)		18.7(9)	2077.5	1050.9
	1061.1(3)		48.9(24)	2112.1	1050.9
	1116.6(3)	Y	5.60(28)	2167.2	1050.9
	1226.8(3)		18.3(9)	2277.7	1050.9
1064.3	114.5(3)		1.23(6)	1541.8	1427.3
	189.1(3)		3.30(16)	1616.4	1427.3
	268.9(3)		2.73(14)	1696.2	1427.3
	308.9(3)		3.28(16)	1736.2+x	1427.3+x
	363.0(3)		100(5)	1427.3	1064.5
	424.6(3)		1.27(6)	1851.9	1427.3
	475.0(3)		0.90(5)	1902.3+x	1427.3+x
	488.2(3)		1.58(8)	1915.5	1427.3
	511.8(3)		12.5(6)	1939.1+x	1427.3+x
	569.6(3)	Y	45.3(23)	1633.9	1064.5
	665.8(3)		5.88(29)	2093.1	1427.3
	790.7(3)		1.44(7)	2218.0	1427.3
	853.8(3)	Y	11.3(6)	1918.0	1427.3
	925.1(3)		3.19(16)	2352.4	1427.3
	1015.1(3)		3.37(17)	2442.4+x	1427.3+x
1121.8	270.1(3)	Y	5.50(27)	1679.3	1409.6
	287.5(3)		100(5)	1409.6	1121.8
	314.9(3)		13.9(7)	1436.7	1121.8
	386.8(3)		48.5(24)	1508.4	1121.8
	462.9(3)		24.8(12)	2077.5	1614.6
	476.5(3)	Y	15.2(8)	1598.3	1121.8
	486.6(3)	Y	13.8(7)	1608.4	1121.8
	492.7(3)		41.0(20)	1614.8	1121.8
	516.2(3)		56.8(28)	1638.0	1121.8
	557.4(3)	Y	20.6(10)	1679.3	1121.8
	596.6(3)	Y	16.4(8)	2033.1	1436.7
	605.1(3)	Y	47.0(23)	1726.8	1121.8
	755.6(3)	Y	20.1(10)	1877.2	1121.8
	796.1(3)	Y	26.5(13)	1918.0	1121.8
	823.2(3)	Y	8.42(42)	1944.7	1121.8
	843.8(3)	Y	11.4(6)	1965.6	1121.8
	906.6(3)		29.6(15)	2028.4	1121.8
	911.1(3)	Y	19.6(10)	2033.1	1121.8
	1015.3(3)	Y	14.8(7)	2137.1	1121.8
	1045.1(3)	Y	39.2(2)	2167.2	1121.8
	1137.6(3)	Y	24.8(12)	2259.4	1121.8
	1155.0(3)	Y	11.3(6)	2276.8	1121.8
	1278.0(3)	Y	11.2(6)	2399.8	1121.8
	1477.7(3)	Y	17.4(9)	2599.5	1121.8
1160.1	248.9(3)		39.7(20)	1409.6	1160.1
	276.5(3)		44.7(22)	1436.7	1160.1
	348.1(3)		33.4(17)	1508.4	1160.1
	356.5(3)		100(5)	1516.6	1160.1
	477.7(3)		28.6(14)	1638.0	1160.1
	976.0(3)	Y	49.6(25)	2136.1	1160.1
	1029.2(3)	Y	85.5(43)	2189.3	1160.1
gs trans	687.0(3)				
	1050.9(3)				
	1064.3(3)				
	1121.8(3)				
	1160.1(3)				
	1181.4(3)				
	1407.6(3)				
	1409.6(3)				
	1436.6(3)				

only if the proper ground-state transition was observed in this coincidence spectrum. In nearly all cases, the newly placed γ rays appeared to be in cascades of multiplicity two.

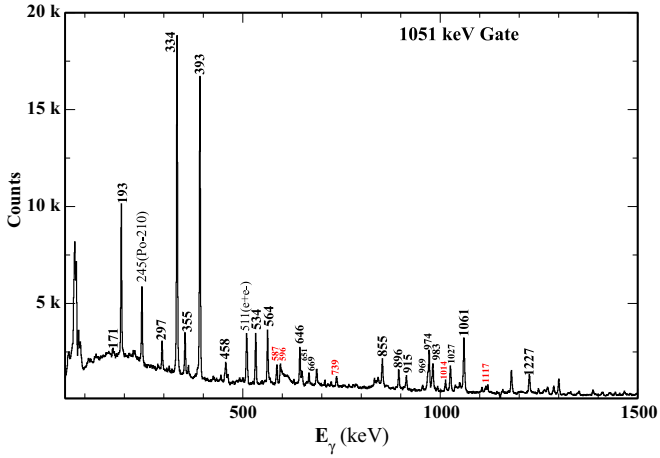

FIG. 1. Spectrum gated on the 1051-keV γ ray. The peaks labeled in red were not observed in previous studies.

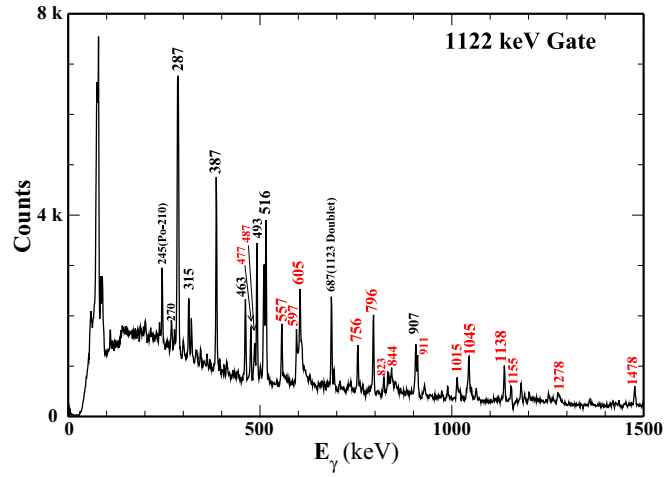

FIG. 3. Spectrum gated on the 1122-keV γ ray.

The eighth ground-state transition in ^{211}Po is the 1181.4-keV transition, which is a doublet with the $2_1^+ \rightarrow 0_{gs}^+$ transition in ^{210}Po. We examined the spectrum gated on the 1181-keV γ ray only to confirm states that had been placed in the level scheme by Fant *et al.* [3].

The γ rays observed in the present experiment are listed in Table I. We have not listed the γ rays in the usual way, that is, by placing all γ rays in a single list ordered by energy. Instead, we have listed the γ rays seen in each ground-state transition coincidence spectrum separately. The γ rays observed in the spectrum gated on the 687.0-keV ground-state transition are listed first; next, those seen in coincidence with the 1050.9-keV transition; and so forth. The γ rays that were not reported in Refs. [3,4] are marked by Y in the table.

The spectra gated on the 1050.9-, 1064.3-, 1121.8-, and 1160.1-keV transitions are shown in Figs. 1, 2, 3, and 4, respectively.

The states assigned to the level scheme are listed in Table II. In several cases, the sum of γ-ray energies in a cascade—that is, the deduced energy of the state being deexcited by the cascade—was within 0.4 keV of the corresponding sum for another cascade. In such a case, we assumed in building the level scheme that the two cascades deexcite the same state. However, there is no way to be sure that this is the case. The two cascades might instead deexcite two distinct states that happen to be nearly degenerate. This is discussed in detail in Secs. VI and VII. Table II also includes four states for which the energies include the notation $+x$. Fant *et al.* [3] found that the time spectrum for the 363-keV γ ray includes both prompt and delayed components. They concluded that there is an isomer of half-life 25 ns that decays to the 1427-keV state (which in turn decays via the 363-keV transition). Fant *et al.* were unable to identify any γ rays that feed this isomer, but McGoram *et al.* [4] identified ten that did. In the (α,n) measurement being reported here, we observed four of the γ rays feeding this isomer. The transition deexciting this isomer has not been identified, so the energy of the isomer is specified in Table II as $1427+x$, and the states observed here that feed the isomer are indicated with an energy that includes $+x$.

The level scheme observed in the present experiment is illustrated in Figs. 5 and 6. In drawing their level scheme,

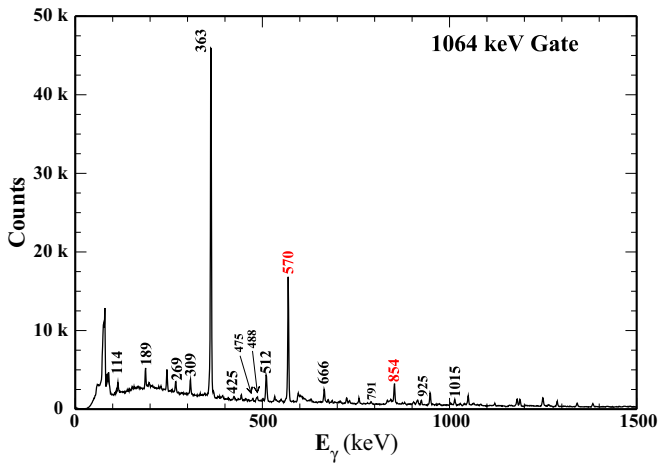

FIG. 2. Spectrum gated on the 1064-keV γ ray.

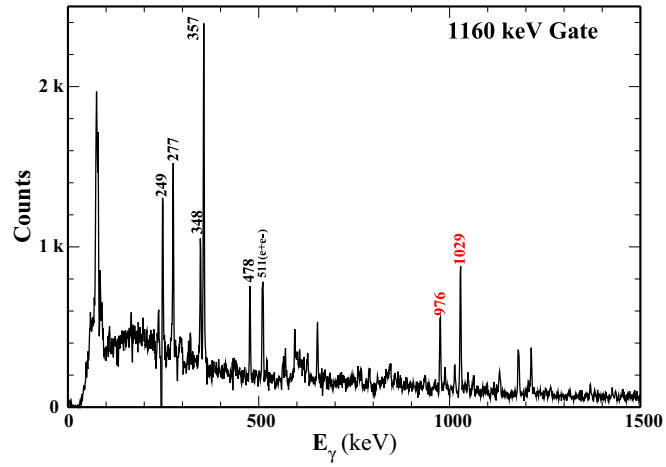

FIG. 4. Spectrum gated on the 1160-keV γ ray.

TABLE II. States observed in the present study.

Energy [keV]	J^π	New
0.0	$9/2^+$	
687.0(3)	$11/2^+$	
1050.9(3)	$5/2^+$	
1064.3(3)	$15/2^-$	
1121.8(3)	$(7/2^+,9/2^+,11/2^+)$	
1160.1(3)	$(7/2^+,9/2^+,11/2^+)$	
1181.4(3)	$(7/2^+,9/2^+,11/2^+)$	
1385.3(3)		
1407.6(3)		
1409.6(3)		
1427.3(3)	$(17/2^+)$	
1427.3(3)+x	$(21/2^+)$	
1436.7(3)		
1443.5(3)		
1459.2(3)		
1508.4(3)		
1508.8(3)		
1516.6(3)		
1541.8(3)		
1578.5(3)		
1584.6(3)		
1598.3(3)		Y
1608.4(3)		Y
1614.8(3)		
1616.4(3)		
1633.9(3)		Y
1638.0(3)		
1647.1(3)		Y
1679.3(3)		Y
1696.2(3)		
1715.7(3)		
1726.8(3)		
1736.2(3)+x		
1740.0(3)		
1789.6(3)	$5/2^+$	Y
1797.4(3)		
1810.0(3)		
1851.9(3)		
1877.2(3)		
1902.3(3)+x		
1915.5(3)		
1918.0(3)		Y
1939.1(3)+x		
1944.7(3)		
1965.6(3)		Y
2024.8(3)		
2028.4(3)		
2033.1(3)		Y
2033.9(3)		
2065.2(3)		Y
2077.5(3)		
2093.1(3)		
2094.8(3)		
2112.1(3)		
2136.1(3)		Y
2137.1(3)		Y
2167.2(3)		Y
2189.3(3)		Y
2218.0(3)		
2224.1(3)		
2259.4(3)		Y
2276.8(3)		Y
2277.7(3)		
2298.1(3)		
2300.6(3)		
2339.7(3)		
2352.4(3)		
2399.8(3)		Y
2442.4(3)+x		
2547.7(3)		
2599.5(3)		Y

Fant *et al.* [3] divided the level scheme into two sections, one for low-spin states and the other for high-spin states. We have done the same, except that the two sections of the level scheme are in two different figures.

IV. STRUCTURE BELOW 1.3 MeV

We begin the discussion by comparing the experimental level structure of ^{211}Po below 1.3 MeV excitation to the results of a shell model calculation using the modified Kuo-Herling interaction of Warburton and Brown [1]. In this energy range, the density of states is low enough to allow a detailed state-by-state comparison of the experimental spectrum and the results of the shell-model calculation. Aside from the previous γ-ray studies [3,4], the primary spectroscopic study we reference here is the ^{210}Po$(d,p)^{211}$Po study reported by Bhatia *et al.* [6].

The details of the shell-model calculation are described in [7]. The model space includes the proton and neutron orbits above ^{208}Pb. The proton orbits included are $h_{9/2}$, $f_{7/2}$, $i_{13/2}$, $f_{5/2}$, $p_{3/2}$, and $p_{1/2}$. The neutron orbits are $g_{9/2}$, $i_{11/2}$, $j_{15/2}$, $d_{5/2}$, $s_{1/2}$, $g_{7/2}$, and $d_{3/2}$. The interaction is an effective realistic interaction, and the single-particle energies are set to reproduce single nucleon stripping reactions on ^{208}Pb.

The comparison of our experimental results to the shell-model results in this energy range is shown in Fig. 7.

Figure 7 also shows the spectrum given by a simple weak coupling scheme in which single-neutron states in ^{209}Pb are coupled to low-lying core states in ^{210}Po. This picture provides a framework for understanding both the experimental level scheme of ^{211}Po and the shell-model calculation, and the discussion below refers to this simple picture.

The ground state of ^{211}Po was measured in ^{210}Po(d,p) to have an $L = 4$ angular distribution and to have a spectroscopic factor of 0.89 for $g_{9/2}$ transfer. Therefore, it was assigned in Ref. [6] to have $J^\pi = 9/2^+$. The shell model calculation reproduces this conclusion, giving a (d,p) spectroscopic factor of 0.91.

The 687.0-keV state is observed strongly in the ^{210}Po(d,p) reaction. The angular distribution observed in that reaction gives $L = 6$, and the cross section gives $S = 0.95$ for $i_{11/2}$ transfer [6]. The shell-model calculation gives the same

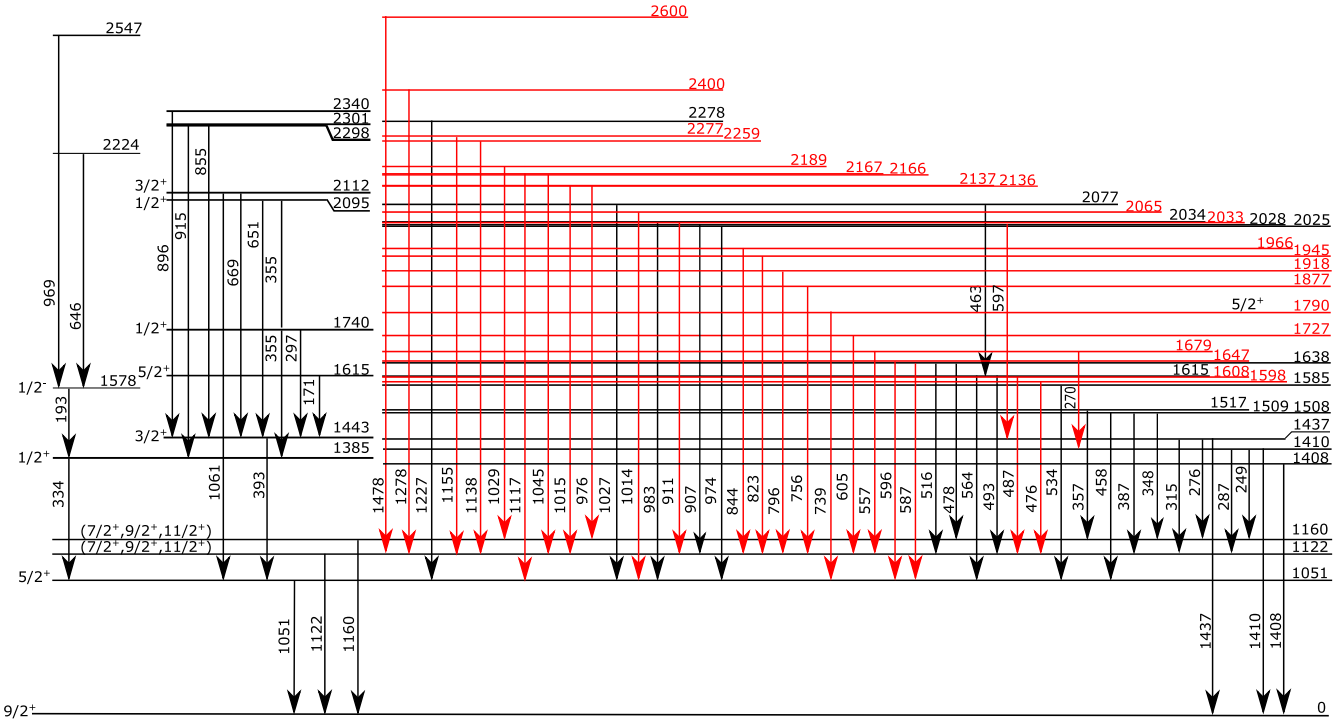

FIG. 5. Low-spin section of the level scheme observed here. The states and transitions drawn in red were not observed in previous studies.

interpretation as an $i_{11/2}$ single neutron state, with an energy of 667 keV and $S = 0.79$. The weak coupling model gives the same interpretation since the $i_{11/2}$ single-neutron state in ^{209}Pb occurs at 779 keV [8].

The next excited state in the experimental spectrum, at 1050.9 keV, is also populated with a significant cross section in the ^{210}Po(d,p) reaction. The (d,p) angular distribution gives $L = 2$ and the spectroscopic factor for $d_{5/2}$ transfer is 0.28 [6], showing that the single-neutron configuration mixes strongly with another $J^\pi = 5/2^+$ configuration. In fact, given that the $2_1{}^+$ state in the core ^{210}Po nucleus occurs at 1181 keV [9], it would be expected that the $5/2^+$ member of the multiplet that results from the coupling of the $g_{9/2}$ neutron to the core $2_1{}^+$ state (and includes states with spins from 5/2 to 13/2) would also occur near this energy. The shell-model calculation predicts that a $5/2^+$ state at 1151 keV contains both a $d_{5/2}$ single neutron component (with $S = 0.25$) and a $g_{9/2} \otimes 2_1{}^+$ component. This is about 100 keV from the observed energy.

According to Ref. [3], the state at 1064.3 keV decays via a stretched $E3$ transition to the ground state, setting $J^\pi = 15/2^-$. The measured half-life of 14.0(2) ns [10] gives $B(E3) = 19.2(9)$ W.u., indicating that this state has a collective octupole component. However, the collective 3^- state in the core ^{210}Po nucleus occurs at a much higher energy (2387 keV). So the 1064.3-keV state in ^{211}Po must have a $j_{15/2}$ single-neutron component as well. This state was not seen in ^{210}Po(d,p) [6] because of the high angular momentum required and the low energy at which the experiment was performed (17.0 MeV). However, in ^{209}Pb there is a $15/2^-$ state with both a $j_{15/2}$ neutron component, with $S = 0.58$ in ^{208}Pb(d,p), and an octupole component (with the $E3$ transition to the $9/2^+$ ground state having $B(E3) = 26(7)$ W.u.) at 1423 keV [8].

Of course, the shell-model calculation does not include a collective octupole state. However, it does predict a $j_{15/2}$ single-neutron state (with $S = 0.72$) at 1194 keV. The shell-model calculation does support the mixing of an octupole component into the experimentally observed state this way: The shell-model calculation gives $B(E3)$ to the ground state of 0.72 W.u. Clearly, the addition of a collective octupole component is necessary to give the observed $E3$ strength.

The structure of the next three states at 1121.8, 1160.1, and 1181.4 keV is much less clear. The 1121.8- and 1160.1-keV states were weakly populated in ^{210}Po(d,p), but no spin information could be obtained from that measurement. All three of these states occur near the energy of the $2_1{}^+$ state in the core ^{210}Po nucleus (1181.4 keV) and all decay to the ground state, so they are likely members of the multiplet resulting from the coupling of the $g_{9/2}$ neutron to the ^{210}Po $2_1{}^+$ state.

The shell-model calculation provides support for this picture by predicting that a set of positive parity states with $J = 5/2,7/2,9/2,11/2$, and 13/2 having strong $E2$ transitions to the $9/2^+$ ground state occurs in the energy range 1124–1435 keV. We have already discussed the $5/2^+$ state in this group, which occurs experimentally at 1050.9 keV and which mixes with the $d_{5/2}$ single-neutron state. The shell model predicts that the three lowest energy members of this group of states are an $11/2^+$ state at 1124 keV, a $9/2^+$ state at 1135 keV, and a $7/2^+$ state at 1136 keV. Therefore, it seems most likely that the experimental states at 1122, 1160, and 1181 keV correspond to these calculated $7/2^+$,$9/2^+$, and $11/2^+$ states. However, there is no convincing experimental evidence for which of the observed states corresponds to each spin.

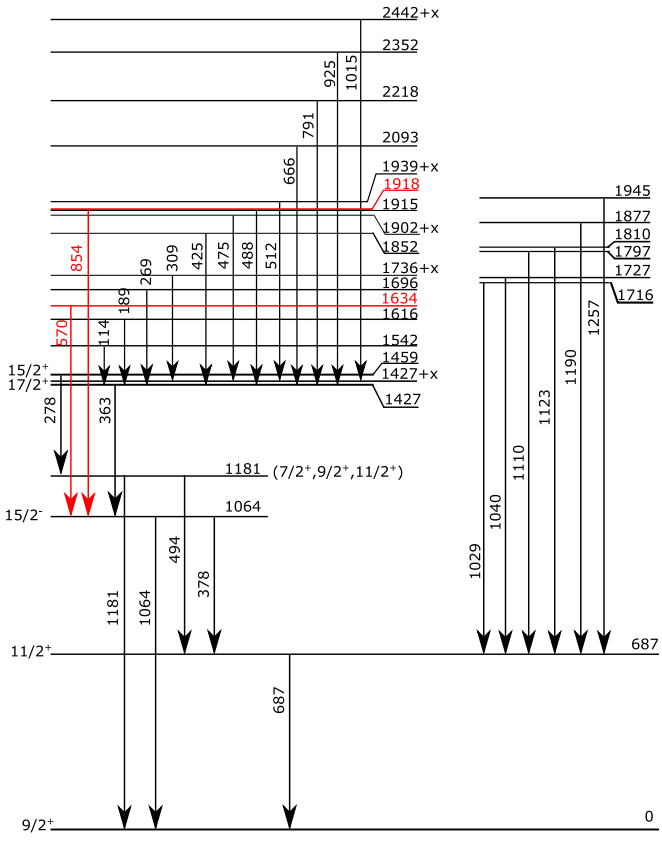

FIG. 6. High-spin section of the level scheme observed here.

Furthermore, we have not yet suggested the location of the $J = 13/2$ member of the $\nu g_{9/2} \otimes 2_1^+$ multiplet, which the shell-model calculation predicts to occur at 1238 keV. It is quite possible that any of the experimental states at 1122, 1160, or 1181 keV could be the $13/2^+$ member of the multiplet, and in fact that was suggested in Ref. [3]. However, that assignment was suggested on the basis of the angular distribution of the 1181-keV γ ray in the singles spectrum, where this transition is a doublet with the 1181 keV $2_1{}^+ \rightarrow 0_{gs}{}^+$ γ ray in ^{210}Po, which is also present in the experiment reported in Ref. [3]. The only conclusion we can draw is that we have observed four of the five members of the $\nu g_{9/2} \otimes 2_1{}^+$ multiplet below 1.4 MeV, and that the fifth must be above 1.4 MeV where the density of states is high so that we cannot identify it. The shell-model calculation predicts that one member of the multiplet is above 1.4 MeV. Furthermore, we have already seen that the calculation predicts energies that vary 100 keV from observed energies, so it should not be surprising that one of the multiplet members would occur above 1.4 MeV and be difficult to identify.

V. STATES OBSERVED IN (α,n) vs (d,p)

We cannot draw conclusions about the structure of each individual state above 1.4 MeV because of the high density of states. However, the ^{210}Po(d,p) experiment [6] populated 13 states between 1.3 MeV and the upper limit of the energy range covered by our (α,n) experiment, which is 2.6 MeV, and the (d,p) data, of course, provide significant information about some of these states. The compilation in Ref. [10] made the connection between the 1385-keV state seen in the γ-ray experiment reported in Ref. [3] (and in the present work) and a state reported in (d,p) at 1378(10) keV to be populated by $L = 2$ transfer. The authors of the (d,p) study [6] assigned this to be an $S = 0.08$ fragment of the $d_{5/2}$ neutron state, but the compiler [10] preferred a $J = 3/2$ assignment (implying $d_{3/2}$ neutron strength rather than $d_{5/2}$). This difference of opinion cannot be resolved given the available information.

A state observed in the (d,p) reaction at 1436(10) keV and tentatively assigned $L = 2$ with $S = 0.05$ for $d_{5/2}$ transfer might correspond to either the 1437- or 1443-keV states observed here (and in Ref. [3]). It cannot correspond to the 1427-keV state because that state has high spin and it decays to the $15/2^-$ 1064-keV state.

The next state observed in (d,p) was at an energy of 1799(10) keV. Its angular distribution indicated $L = 2$ transfer and the cross section gave $S = 0.40$ for $d_{5/2}$ transfer. The only state observed in either prior γ-ray experiment in the energy range 1789–1809 keV was the 1797-keV state that decays to the 687-keV $11/2^+$ state, so this state is too high in spin to correspond to the state observed in (d,p). However, in the present experiment we observed a state at 1790 keV that decays via a 739-keV γ ray to the 1051-keV $5/2^+$ state, and we confidently assign our 1790-keV state to be the $d_{5/2}$ state seen with the (d,p) reaction. In fact, the shell-model calculation predicts that the strongest $d_{5/2}$ state—having $S = 0.53$—occurs in a state at 1885 keV. Therefore, the experimentally observed 1790-keV state appears to correspond to the predicted 1885-keV $5/2^+$ state.

It was pointed out previously [10] that the states observed in (d,p) at 2022(10) and 2084(10) keV could each correspond to several states seen in the previous (α,n) study [3] as well as in the present study. The state observed in (d,p) at 2161(10) keV was not seen by Fant *et al.* [3]. However, in the present study we observe a state at 2167 keV that matches the energy in the (d,p) experiment. The authors of the (d,p) study [6] tentatively assigned this state to have $J^\pi = 1/2^+$.

The next state observed in (d,p), at 2315(10) keV, may correspond to either of the states observed at 2298 and 2300 keV in both the present and previous [3] (α,n) studies. However, there is no state seen in the (α,n) studies that could correspond to the 2364(10) keV state seen in (d,p).

The last five states seen in (d,p) within the energy range observed in the present (α,n) experiment (up to 2.6 MeV) were seen at 2390(10), 2414(10), 2456(10), 2560(10), and 2606(10) keV. Either of the 2390(10) or 2414(10) keV (d,p) states might correspond to the 2400-keV state observed in the present study for the first time. There are no states in the present study that could correspond to the 2456(10)- or 2560(10)-keV states. However, the 2606(10)-keV (d,p) state might correspond to the 2600-keV state seen in the present study.

VI. COMPLETE SPECTROSCOPY BELOW 2.0 MeV

We now address the question of whether the shell-model calculation presented here can reproduce the number of states

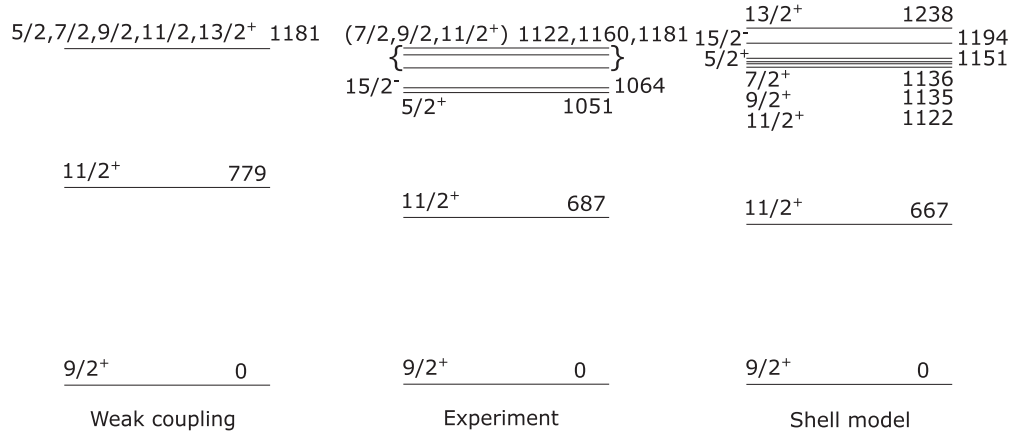

FIG. 7. States observed below 1.3 MeV compared to those calculated in the same energy range in the shell-model calculations described here and using a weak coupling scheme.

observed in the present study below 2.0 MeV. We limit our analysis to energies below 2.0 MeV to mostly exclude the collective octupole state, which is not included in the shell-model calculation. In the core ^{210}Po nucleus, the 3_1^- state is located at 2387 keV [9].

In the present (α,n) experiment, we observed 45 states (including the ground state) below 2.0 MeV. There are two qualifications to that statement. First, we observed two γ rays deexciting a state at 1679 keV. We assume that these two γ rays deexcite a single state. However, it is possible that each of these two γ rays deexcites a different state and that the two states are within a few tenths of a keV in energy. To prove conclusively that it is a single state, we would need to observe a γ ray that populates the state in the coincidence gates on each γ ray. We do not see such a γ ray (not surprisingly because the experiment is dominated by cascades of multiplicity two) so it remains possible that there are two states at 1679 keV instead of one. Similar situations exist for the 1727-, 1877-, 1918-, and 1945-keV states. Given that, it is possible that we have observed 50 states below 2.0 MeV instead of just 45.

Second, among the 45 states we list below 2.0 MeV, there are four (listed in Table II as $1427+x$, $1736+x$, $1902+x$, and $1939+x$) that are associated with an isomer of half-life 25 ns and of unknown energy that decays to the 1427-keV state. This was discussed in Sec. III. It seems likely that x is quite small since a higher energy transition would probably not give as long a half-life. Our shell-model calculation supports this supposition. The observed 1427-keV state has tentatively been assigned $J^\pi = 17/2^+$. The shell-model calculation gives the corresponding $17/2^+$ state to be at 1480 keV, and a $21/2^+$ state only 25 keV higher at 1505 keV. Clearly, that yrast $21/2^+$ state would decay isomerically to the $17/2^+$ state. Therefore, based on the shell-model calculation, we estimate that $x = 25$ keV. We conclude that all four of the $+x$ states we observe are likely to be located under 2.0 MeV.

Our shell-model calculation predicts 52 states with energies under 2.0 MeV (including the ground state). However, these 52 states include some with spins higher than could be observed using the present reaction. The 52 calculated states include a $31/2^-$ state at 1946 keV (probably corresponding to a state observed in the light heavy-ion-induced reaction of Ref. [4] at 2136 keV), a $23/2^+$ state at 1878 keV, a $27/2^+$ state at 1807 keV (probably corresponding to the 1820-keV state observed in Ref. [4]), a $25/2^+$ state at 1726 keV, a $23/2^+$ state at 1643 keV, and a $25/2^+$ state at 1499 keV, which corresponds to the 25-s isomer at 1462 keV that α decays 99.984% of the time [10].

Our experimental results support the assertion that we do not see states with $J > 21/2$ with the present reaction. Using light heavy-ion-induced reactions, McGoram *et al.* [4] observed ten γ rays that decay (either directly or in cascade) to the $1427+x$ state. We observed four of those γ rays (309, 475, 512, and 1015 keV). As explained above, it is likely that the $1427+x$ state has $J^\pi = 21/2^+$. It is therefore likely that the states observed by McGoram *et al.* to decay to the $1427+x$ state have $J = 25/2$ or lower. Furthermore, since we see some of these states but not all, it is likely that the states we do not see are the states among these that have the highest spins. It is almost certain that we do not see states with $J = 25/2$, and it is quite likely that we also do not see states with $J = 23/2$.

A calculation of the ^{208}Pb$(\alpha,n)^{211}$Po reaction at 24 MeV (the beam energy and the maximum energy at which reactions occur in the thick target used here) using the fusion-evaporation code PACE [11] provides support for this argument by showing how the partial cross sections for different J values falls off quickly as spin increases beyond the grazing angular momentum of $7\hbar$. For $J = 6$, the partial cross section is calculated to be 57 mb, while for $J = 7$ it is 53 mb. By $J = 11$, the partial cross section has dropped to 19 mb, and for $J = 12$, it is 13 mb.

If we delete the six states calculated by the shell model to occur below 2.0 MeV in energy and to have $J > 21/2$, then we arrive at a prediction that we should observe 46 states in this energy range (including the ground state), quite close to the observed number of 45.

Not only does the shell-model calculation reproduce the total number of states in this spin ($J \leqslant 21/2$) and energy ($\leqslant$2.0 MeV) range with precision, but it also reproduces in detail the density of states as the excitation energy increases. Figure 8 shows the accumulated number of states as a function of excitation energy observed in the experiment and calculated using the shell model and the weak coupling scheme up to

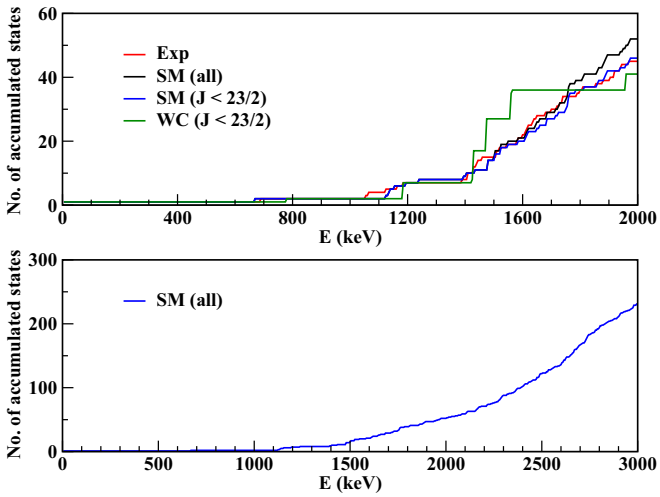

FIG. 8. Number of accumulated states observed in the experiment and for shell model and weak coupling calculations. The upper panel, which shows states up to 2.0 MeV, includes two shell-model lines: one for all states calculated using the shell model and the other excluding states having $J = 23/2$ or higher. The weak coupling line excludes states having $J = 23/2$ or higher. The lower panel shows all shell model states up to 3.0 MeV.

2.0 MeV (upper panel) and for just the shell model up to 3.0 MeV (lower panel). That is, the 1000-keV point in the plot shows the total number of states at 1000 keV or below. The upper panel includes two lines for the shell-model calculation, one that includes all calculated states and a second that excludes calculated states with $J \geqslant 23/2$. The weak coupling line also excludes states with $J \geqslant 23/2$.

The shell-model line in the upper panel of Fig. 8 including only states with $J \leqslant 21/2$ reproduces the experimental line in detail. This success is not surprising given the decades of refinements that have been invested in shell-model calculations near ^{208}Pb. The lower panel shows the increasing density of states with increasing excitation energy. While there are only 52 states predicted by the shell model to occur at all spins at 2.0 MeV and below, an additional 179 are predicted to occur between 2.0 and 3.0 MeV.

It is important to note that in the same energy and spin range, the previous study of the ^{208}Pb$(\alpha,n)^{211}$Po reaction by Fant *et al.* [3] observed only 32 states. Two factors contribute to the improvement in the present study. First, Fant *et al.* ran their experiment with a beam energy of 20.6 MeV, very close to the Coulomb barrier and certainly with a smaller cross section. Second, the detectors used in the present experiment are considerably more sensitive than those used by Fant *et al.*, which were small volume Ge(Li) detectors without Compton suppression.

VII. STRUCTURE ABOVE 2.0 MeV

In the present experiment, we observed 18 states above 2.0 MeV. As was the case below 2.0 MeV, there are several states we list in Table II that may in fact each be two states that are nearly degenerate at 2033, 2078, and 2167 keV. If that is true, then the number of states we observed above 2.0 MeV is actually larger than 18. Of these 18 states, 8 have not been previously observed in γ-ray experiments. However, as described in Sec. V, two of these new states probably correspond to states seen in the ^{210}Po$(d,p)^{211}$Po reaction.

VIII. SUMMARY

Using the ^{208}Pb$(\alpha,n)^{211}$Po reaction at 24 MeV with a thick target, we observed 26 γ rays and 18 states that had not been previously observed in γ-ray studies.

We used these results to test whether a Kuo-Herling shell model calculation can reproduce the number of states observed below 2.0 MeV and at spins of 21/2 and below. We observed 45 states in this energy and spin range, while the calculation predicted that 46 such states would occur.

ACKNOWLEDGMENT

This work was supported by the National Science Foundation under Grant No. 14-01574.

[1] E. K. Warburton and B. A. Brown, Phys. Rev. C **43**, 602 (1991).
[2] A. Dewald, R. Reinhardt, J. Panqueva, K. O. Zell, and P. von Brentano, Zeitschr. Phys. A **315**, 77 (1984).
[3] B. Fant, T. Lonnroth, and V. Rahkonen, Nucl. Phys. A **355**, 171 (1981).
[4] T. McGoram, G. Dracoulis, A. Byrne, A. Poletti, and S. Bayer, Nucl. Phys. A **637**, 469 (1998).
[5] J. R. Pavan, Structure of ^{87}Nb and ^{22}F, Ph.D. thesis, Florida State University, Tallahassee, Florida, 2004 (unpublished).
[6] T. Bhatia, T. Canada, P. Barnes, R. Eisenstein, and C. Ellegaard, Nucl. Phys. A **314**, 101 (1979).
[7] E. K. Warburton, Phys. Rev. C **44**, 1500 (1991).
[8] J. Chen and F. G. Kondev, Nucl. Data Sheets **126**, 373 (2015).
[9] M. S. Basunia, Nucl. Data Sheets **121**, 561 (2014).
[10] B. Singh, D. Abriola, C. Baglin, V. Demetriou, T. Johnson, E. McCutchan, G. Mukherjee, S. Singh, A. Sonzogni, and J. Tuli, Nucl. Data Sheets **114**, 661 (2013).
[11] O. Tarasov and D. Bazin, Nucl. Instr. Methods Phys. Res. B **204**, 174 (2003).